A theoretical analysis of nonsteady-state oxygen transfer in layers of hemoglobin solution

Pflügers Arch. 384, 231–239 (1980)

Pflügers Archiv
European Journal of Physiology

A Theoretical Analysis of Nonsteady-State Oxygen Transfer in Layers of Hemoglobin Solution*

J. A. E. Spaan[1], F. Kreuzer[2], and L. Hoofd[2]

[1] Department of Physiology and Physiological Physics, Leiden University Medical Center, Wassenaarseweg 62, Leiden
[2] Department of Physiology, University of Nijmegen, Geert Grooteplein Noord 21a, Nijmegen, The Netherlands

Abstract. The oxygenation of layers of hemoglobin solutions thick enough to ensure chemical equilibrium between oxygen and hemoglobin has been analyzed theoretically assuming simultaneous diffusion of oxygen and oxyhemoglobin. The dimensionless transfer equation was solved for the finite and semi-infinite situation, the parameters being 1) the ratio of bound to physically dissolved oxygen after equilibration (H), 2) the ratio of carrier-mediated to free oxygen flux at steady state (D^*), and 3) the dimensionless saturation curve (characterized by Φ_{50}). A parametric analysis provided plots of the dimensionless oxygenation time against these three dimensionless parameters. In this way, from the oxygenation times plotted as a function of the reciprocal oxygen driving pressure in any particular hemoglobin solution, the values of the oxygen permeability (or, knowing oxygen solubility, of the oxygen diffusion coefficient) and of the hemoglobin diffusion coefficient can be derived simultaneously.

Key words: Oxygen – Hemoglobin – Diffusion – Facilitated diffusion – Diffusion coefficient of oxygen and hemoglobin.

Introduction

The theoretical and experimental investigation of the nonsteady-state oxygenation of layers of hemoglobin-containing media is important for many problems of oxygen uptake in the organism as well as in artificial oxygenators. Since the blood is heterogeneous and has a relatively constant composition, studies of hemoglobin solutions varying in concentration provide a simpler situation covering a wider range of conditions.

The group of Fribourg introduced the thin-layer technique with photometric recording of oxygenation some thirty years ago (review by Kreuzer, 1953). Klug et al. (1956), using the advancing front method, determined the oxygen diffusion coefficient in highly concentrated hemoglobin solution, while taking into account the contribution by the simultaneous diffusion of oxyhemoglobin over the entire range of hemoglobin concentrations for the first time. These studies were extended and confirmed by Kutchai (1971a, b) who, however, concluded that oxygen diffusion facilitated by oxyhemoglobin was of minor importance only. Spaan (1973) used advancing front equations corrected for the physically dissolved oxygen, and suggested a facilitating contribution by oxyhemoglobin and a possibility of determining values of both oxygen and hemoglobin diffusion coefficients from oxygenation experiments.

Thews (1957) applied an approximate solution of the diffusion equations based on simplifying assumptions to the data of Kreuzer (1950) and Klug et al. (1956) and found good agreement of the values of the oxygen diffusion coefficient between his calculations and previous approaches where a comparison was possible. He neglected, however, the simultaneous diffusion of oxyhemoglobin, as did later studies by Marx et al. (1960), Weissman and Mockros (1969), Dindorf et al. (1971), and Mikic et al. (1972). Moll (1968/69), using numerical methods, on the other hand evaluated the acceleration of oxygen uptake and release by oxyhemoglobin diffusion in red cells.

It is the purpose of the present work to theoretically analyze the oxygenation of hemoglobin solution layers including its facilitation by the simultaneous diffusion of oxyhemoglobin, to compare the theoretical results with new experimental data, and to simultaneously derive the values of the diffusion coefficients of oxygen and hemoglobin over a wide range of hemoglobin

* Most of this work was performed when the first author was employed at the Biomedical Engineering Section of the Department of Production Engineering, Eindhoven University of Technology, Eindhoven, The Netherlands

0031-6768/80/0384/0231/$01.80

solution concentrations in the presence of varying oxygen driving pressures. As may be deduced from the short survey of the literature summarized above, this has never been done before.

In the present first, theoretical, paper the basic relationships are derived based on the diffusion equations for both oxygen and hemoglobin, assuming chemical equilibrium between oxygen and hemoglobin. In a second, companion paper the experimental methods and results will be presented and the most important factors will be derived and discussed.

The Oxygenation of Hemoglobin Layers of Finite or Semi-Infinite Thickness and the Definition of the Oxygenation Time

A finite thickness of a flat layer of hemoglobin solution is at one side ($x = 0$) exposed to a gaseous atmosphere and at the other side ($x = d$) limited by a gas-impermeable wall. At time $t < 0$ the layer is in equilibrium with oxygen at a partial pressure P_i. The oxygen concentration all over the layer equals C_i according to Henry's law and the oxygen saturation equals S_i as required by the oxygen saturation curve. At time $t = 0$ the gaseous atmosphere is changed abruptly to a P_{O_2} value of P_1. Oxygen will diffuse into the hemoglobin layer and react with hemoglobin to produce oxyhemoglobin. We will assume that the reaction of oxygen with hemoglobin is infinitely fast. The transfer equation describing this oxygenation process (Spaan, 1973) is in dimensionless form:

$$\frac{\partial}{\partial t^*}(\Phi + H\,\Psi) = \frac{\partial^2 \Phi}{\partial x^{*2}} + D^* \frac{\partial^2 \Psi}{\partial x^{*2}} \tag{1}$$

where (see also List of Symbols):

$t^* = \dfrac{tD_C}{d^2}$ = dimensionless time

t = time (s)

D_C = diffusion coefficient of dissolved oxygen ($\mu m^2/ms$)

$x^* = x/d$ = dimensionless distance from liquid-gas interface

x = distance from liquid-gas interface (μm)

d = layer thickness (μm)

$\Phi = \dfrac{C - C_i}{C_1 - C_i}$ = dimensionless oxygen concentration

$C_i = \alpha P_i$ = initial oxygen concentration (mol/l)

α = solubility of oxygen in the solution (mol/l/kPa)

P_i = initial oxygen partial pressure (kPa)

$C_1 = \alpha P_1$ = final oxygen concentration (mol/l)

P_1 = final oxygen partial pressure or oxygen driving pressure (kPa)

$\Psi = \dfrac{S - S_i}{S_1 - S_i}$ = dimensionless oxygen saturation

S_i = initial oxygen saturation (fractional)

S_1 = final oxygen saturation (fractional)

$H = \dfrac{(S_1 - S_i)h}{(C_1 - C_i)}$ = oxygen concentration ratio = ratio of bound to physically dissolved oxygen after equilibration

h = total oxygen binding capacity of the hemoglobin solution (mol/l)

$D^* = H\dfrac{D_H}{D_C}$ = oxygen flux ratio = ratio of carrier-mediated to free oxygen flux at steady state

D_H = diffusion coefficient of hemoglobin ($\mu m^2/ms$).

The advantage of the dimensionless analysis is that only three parameters are involved (H, D^*, and a parameter defining the dimensionless saturation curve), whereas eight are necessary in the analysis with dimensions (D_C, d, P_i, P_1, α, h, D_H, and a parameter defining the saturation curve).

The boundary conditions for the finite layer problem are:

$$\begin{aligned} &t^* = 0; && 0 < x^* \leq 1; && \Psi = \Phi = 0 \\ &t^* \geq 0; && x^* = 0; && \Psi = \Phi = 1 \\ &t^* \geq 0; && x^* = 1; && \frac{\partial \Phi}{\partial x^*} = \frac{\partial \Psi}{\partial x^*} = 0. \end{aligned} \tag{2}$$

Profiles of oxygen saturation and oxygen concentration in a finite slab calculated from eqs. (1) and (2) were presented previously (Spaan, 1973). If the hemoglobin is not mobile the saturation profile in general shows a quite steep course, and the profiles are steeper at higher values of P_1. When hemoglobin is mobile the profiles become smoother, particularly at lower values of P_1.

In the early phase of the oxygenation process oxygen will not have penetrated into the layer far enough for the boundary conditions at $x^* = 1$ to influence significantly the distribution of physically dissolved and chemically bound oxygen. Hence one may expect the oxygen uptake of a layer with finite thickness ($x^* = 1$) to be similar to a layer extending into infinity ($x^* \to \infty$) during this early phase. Note that for this semi-infinite layer the space coordinate x has been normalized by dividing by the thickness of the finite layer. For the semi-infinite model the third boundary condition of eq. (2) no longer holds and has to be replaced by:

$$x^* \to \infty : \Phi \to 0 \text{ and } \Psi \to 0. \tag{3}$$

It is well known from the analysis of mass and heat transfer problems that for the case of a semi-infinite layer the solution of eq. (1) can be found as a function of only one independent variable η defined by:

$$\eta = \frac{x^*}{\sqrt{t^*}};\ t^* > 0,\ x^* \geq 0. \tag{4}$$

Equation (1) can now be rewritten as a function of η (see Appendix for derivation):

$$-\tfrac{1}{2}\,\eta\,\frac{d}{d\eta}(\Phi + H\,\Psi) = \frac{d^2\Phi}{d\eta^2} + D^*\,\frac{d^2\Psi}{d\eta^2}. \tag{5}$$

The boundary conditions become:

$$\eta = 0;\ \Phi = \Psi = 1$$
$$\eta \to \infty;\ \Phi \to 0 \text{ and } \Psi \to 0. \tag{6}$$

This study mainly concerns the increase of the average oxygen saturation when oxygenating hemoglobin layers. The average dimensionless saturation of a finite slab $[\bar{\Psi}(t^*)]$ is defined by the ratio of the amount of oxygen already bound to hemoglobin and the maximal amount of oxygen that can be bound to hemoglobin in the layer. This leads to:

$$\bar{\Psi}(t^*) = \int_0^1 \Psi(x^*, t^*)\,dx^*. \tag{7}$$

In this equation Ψ is to be calculated by the finite layer model [boundary conditions of eq. (2)]. However, since during the initial phase Ψ can also be calculated by the semi-infinite layer model, and Ψ will be practically zero for $x^* > 1$, eq. (7) can be rewritten to:

$$\bar{\Psi}_\infty(t^*) = \int_0^\infty \Psi_\infty\left(\frac{x^*}{\sqrt{t^*}}\right) dx^*. \tag{8}$$

The index ∞ indicates that $\Psi_\infty(\eta)$ $\left(=\Psi_\infty\left(\frac{x^*}{\sqrt{t^*}}\right)\right)$ and $\bar{\Psi}_\infty(t^*)$ have been calculated with the semi-infinite model. Obviously we have to restrict the value of $\bar{\Psi}_\infty(t^*)$ to the physically significant range of $0 \le \bar{\Psi}_\infty(t^*) \le 1$. With the aid of eq. (4), eq. (8) can be rewritten:

$$\bar{\Psi}_\infty(t^*) = \sqrt{t^*}\,\{\int_0^\infty \Psi_\infty(\eta)\,d\eta\}. \tag{9}$$

The integral in brackets is independent of time. Hence, according to the semi-infinite model the average saturation has to increase proportionally to the square root of time. For the finite layer this general conclusion only holds as far as the solutions of the finite and semi-infinite layer coincide.

The oxygenation increases of the finite and semi-infinite model are compared in Fig. 1. The range of coincidence of the solutions of both models is considerable and tends to increase as P_1 is higher. This range of coincidence is controlled by the same conditions that make the saturation profile within the layer steeper. This is understandable because the steeper the saturation profile, the longer the profile is "not aware" of the dimension of the layer.

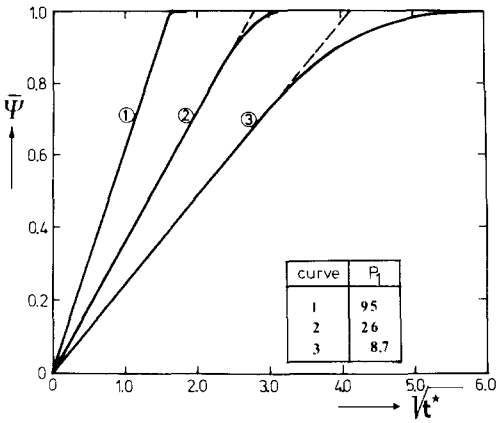

Fig. 1. Oxygenation (average dimensionless oxygen saturation $\bar{\Psi}$) of a finite slab as a function of $\sqrt{t^*}$ ($\bar{\Psi}_d$, solid lines) and according to the semi-infinite slab model ($\bar{\Psi}_\infty$, broken lines). Oxygen binding capacity $h = 6.22 \cdot 10^{-3}$ mol/l ([Hb] = 100 g/l), $D_H/D_C = 0.0281$, $\alpha = 11.4 \cdot 10^{-9}$ mol · l^{-1} · Pa^{-1}. The oxygen driving pressure P_1 is expressed in units of kPa (1 kPa = 7.5 mm Hg). The finite slab oxygenation was calculated numerically according to Spaan (1973)

Therefore it is permitted to apply the semi-infinite solution throughout a large part of the oxygenation process in layers with finite thickness. During this part of the oxygenation process the average dimensionless saturation increases proportionally to the square root of time as measured continuously over the whole range:

$$\bar{\Psi}_\infty(t^*) = \sqrt{\frac{t^*}{t_1^*}} = \sqrt{\frac{t}{t_1}} = \sqrt{\frac{t/d^2}{t_1/d^2}} \tag{10}$$

where t_1^* = dimensionless oxygenation time
t_1 = oxygenation time
t_1/d^2 = normalized oxygenation time.

These three interrelated quantities have been defined since t_1^* is relevant for the dimensionless analysis, t_1 represents the actual oxygenation time of a hemoglobin layer, and t_1/d^2 will be the quantity independent of layer thickness to be measured. Combination of eqs. (9) and (10) results in:

$$t_1^* = 1/\{\int_0^\infty \Psi_\infty(\eta)\,d\eta\}^2. \tag{11}$$

In the following section a parametric analysis will be performed to evaluate the dependence of t_1^* on the oxygen concentration ratio (H), oxygen diffusion ratio (D^*) and dimensionless saturation curve ($\Psi = \Psi(\Phi)$).

The dimensionless dissociation curve is characterized by Φ_{50}, the value of Φ for $\Psi = 0.5$. This Φ_{50} is defined by P_{50}/P_1 as long as P_1 is large enough to ensure that $S_1 = 1$. Thus with $P_{50} = 3.55$ kPa (26.6 mm Hg) for the standard dissociation curve a series of curves is obtained for various values of P_1 (Fig. 2). In case of

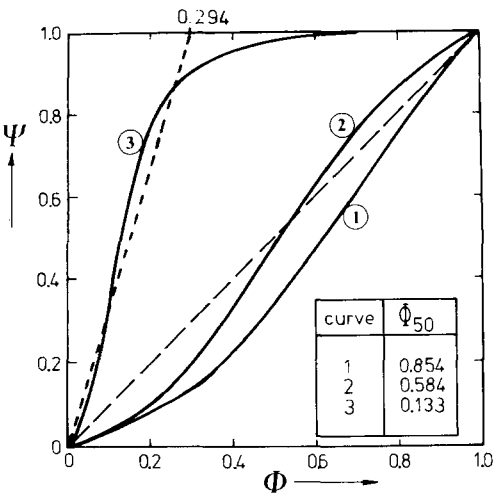

Fig. 2. Dimensionless saturation curves (Ψ versus Φ; $P_i = 0$, $\Psi = S/S_1$, $\Phi = P/P_1$) at several values of Φ_{50}. Every dimensionless saturation curve is obtained from the standard saturation curve and the boundary values P_1 and S_1. The broken line at the right represents a linear approximation of curve 2, the broken line at the left represents part of the polygonal approximation of curve 3

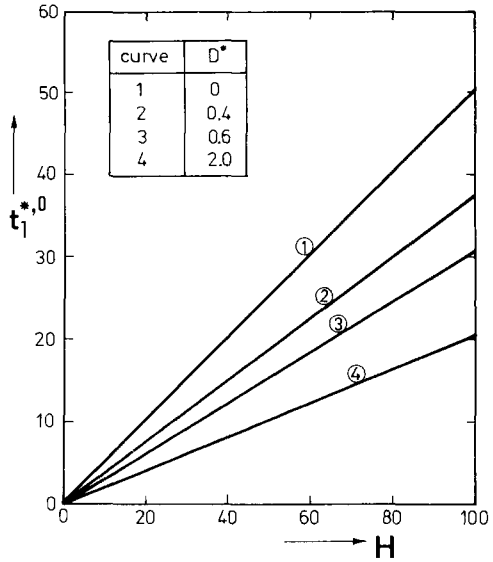

Fig. 3. Dimensionless oxygenation time using a rectangular saturation curve ($= t_1^{*,0}$) as a function of the oxygen concentration ratio (H) for four different values of the oxygen flux ratio (D^*). The intercepts of the curve with the ordinate are close to zero ($t_1^{*,0} \simeq 0.15$)

$S_i = 0$ and P_1 so large that $S_1 = 1$ the dimensionless saturation curve will have the same shape as the real dissociation curve. When, however, P_1 becomes so small or P_{50} so large that S_1 is significantly below unity the dimensionless saturation curve will change in shape and $\Phi_{50} = P_{50}/P_1$ no longer holds. As long as $S_1 = 1$ the dimensionless saturation curve will be shifted by a change of P_1, as it will by changing pH, P_{CO_2} or temperature shifting the real dissociation curve. In Fig. 2 three curves are shown for Φ_{50} of 0.854 ($P_1 = 4.14$ kPa or 31.1 mm Hg), 0.584 ($P_1 = 6.08$ kPa or 45.5 mm Hg), and 0.133 ($P_1 = 26.7$ kPa or 200 mm Hg), P_{50} always being 3.55 kPa (26.6 mm Hg).

Parametric Analysis

A rectangular saturation curve ($\Phi_{50} = 0$) implies the situation of a sharp advancing saturation front. We first studied the influence of both D^* and H on t_1^* assuming a rectangular saturation curve and using the moving boundary model of Hill (1928/1929). The dimensionless oxygenation time obtained with this type of curve will be denoted by $t_1^{*,0}$ since it forms a certain standard for the oxygenation process at specific values of H and D^*. The effects of the saturation curve and of the diffusion of hemoglobin on the dimensionless oxygenation time will be expressed by two factors f_1 and f_2 respectively. Since it appeared that the role of factor f_2 is easily defined for the rectangular saturation curve, f_2 will be discussed first.

Figure 3 shows that $t_1^{*,0}$ is a linear function of H at constant D^*. The intercept of the curves with the vertical axis is close to zero ($t_1^* \simeq 0.15$). In case of $D^* = 0$ the slope is 0.5 in accordance with the advancing front equation not corrected for physically dissolved oxygen (e.g., Spaan, 1973). Neglecting the small intercept of the curves at $H = 0$ one may describe the curves of Fig. 3 by:

$$t_1^{*,0} = \tfrac{1}{2} f_2 H, \tag{12}$$

where $\frac{1}{2}f_2$ is the slope of these curves and depends on D^*. Indeed, f_2 can be considered as the nonsteady-state facilitation factor reflecting in a reduction of the oxygenation time due to diffusion of hemoglobin.

The nonsteady-state facilitation factor f_2 is plotted in Fig. 4 as a function of D^*. The curve of f_2 versus D^* approaches an hyperbolic shape as indicated by the broken line. For $D^* = 0$ (no facilitation) $f_2 = 1$. The total steady-state oxygen flux with boundary conditions at $x^* = 0$ and $x^* = 1$ corresponding to the nonsteady-state situation at $t^* \geq 0$ and $t^* < 0$ respectively is (e.g. Kreuzer and Hoofd, 1970, 1972):

$$\alpha D_C \Delta P + h\, D_H \Delta S = \alpha D_C \Delta P \left(1 + \frac{h D_H \Delta S}{\alpha D_C \Delta P}\right) = \alpha D_C \Delta P\,(1 + D^*). \tag{13}$$

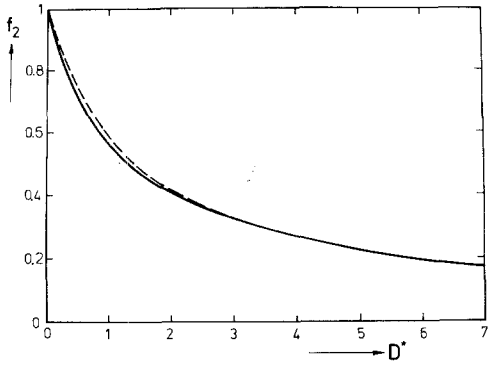

Fig. 4. The nonsteady-state facilitation factor f_2, being twice the tangent of the relationship between the dimensionless oxygenation time, using a rectangular saturation curve ($t_1^{*,0}$), and the oxygen concentration ratio (H) (Fig. 3), as a function of oxygen diffusion ratio D^* ($= H\ D_H/D_C$) (solid line). The f_2 versus D^* curve has an hyperbolic shape and can be approximated (broken line) by $f_2 = 1/(0.690\ D^* + 1)$

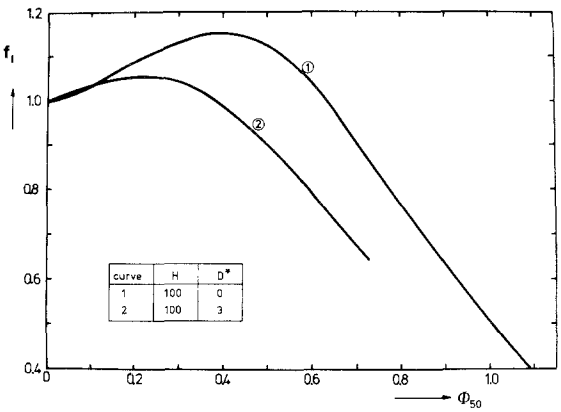

Fig. 5. f_1 ($= t_1^*/t_1^{*,0}$) as a function of Φ_{50}; $t_1^{*,0}$ is the dimensionless oxygenation time for a rectangular saturation curve; Φ_{50} characterizes the dimensionless saturation curve. Initially f_1 and thus the dimensionless oxygenation time t_1^* increase and thereafter decrease with increasing Φ_{50}. This behavior is due to the shape of the saturation curve. Curves *1* and *2* differ in the value of D^* (0 or 3 respectively)

So in fact Fig. 4 relates the nonsteady-state facilitation to the steady-state facilitation.

The influence of the dimensionless saturation curve on the oxygenation time has been studied by plotting the ratio $t_1^*/t_1^{*,0}$, called f_1, as a function of Φ_{50} with D^* and H as parameters. The oxygenation time t_1^* was calculated by the semi-infinite layer model. Figure 5 presents two curves for $H = 100$ and $D^* = 0$ or $D^* = 3$ respectively. The ratio f_1 first increases and then decreases with increasing Φ_{50} due to the change in shape of the dimensionless saturation curve when Φ_{50} increases as shown in Fig. 2 and depends on D^* except at Φ_{50} values below about 0.1. The relationship between f_1 and Φ_{50} for a given value of D^* is affected by H varying from 0 to 500 by no more than 10%.

Table 1. Dependence of f_1 ($= t_1^*/t_1^{*,0}$) on Φ_{50} for three ranges of parameter values of H and D^*. Within these ranges the relationship between f_1 and Φ_{50} varies with H and D^* within the limits indicated in the table

Φ_{50}	$25 \le H \le 100$ $0.2 \le D^* \le 0.8$	$H = 5$ $0.2 \le D^* \le 0.8$	$25 \le H \le 175$ $D^* = 0$
	$f_1 \pm 0.004$	$f_1 \pm 0.009$	$f_1 \pm 0.002$
0.0191	1.012	1.017	1.002
0.0382	1.018	1.023	1.004
0.0535	1.031	1.043	1.015
0.0891	1.055	1.079	1.029
0.1337	1.077	1.119	1.053
0.2026	1.108	1.181	1.094

The influence of H and D^* on the relationship between f_1 and Φ_{50} was studied in more detail for H varying between 5 and 175, D^* varying between 0 and 2, and Φ_{50} varying between 0.019 and 0.203. In absolute terms these ranges correspond to hemoglobin concentrations between $7.7 \cdot 10^{-4}$ mol/l ([Hb] = 50 g/l) and $4.65 \cdot 10^{-3}$ mol/l ([Hb] = 300 g/l). When the P_{50} of the saturation curve equals 1.6 kPa (12 mm Hg), as was the case in our experiments, the range of Φ_{50} corresponds to P_1 values in the range of 8.3 and 95.8 kPa (62.5 and 720 mm Hg). The results are presented in Table 1 and demonstrate that in the range studied both D^* and H have only a minor influence on the relationship between f_1 and Φ_{50}.

Figure 5 shows that for $\Phi_{50} \to 0$ the numerical solution of the differential equation of the semi-infinite model converges to the solution of the moving boundary equation of Hill (1928/1929) using a rectangular saturation curve as expected ($f_1 = 1$).

These results may be summarized by the following implicit formula:

$$t_1^* = \tfrac{1}{2} f_1(\Phi_{50}, H, D^*)\, f_2(D^*)\, H. \tag{14}$$

Thus the dimensionless oxygenation time may be expressed as a product of three factors, the oxygen concentration ratio H, the nonsteady-state facilitation factor f_2 and a factor f_1 describing the influence of the dimensionless saturation curve.

A Strategy for the Experimental Determination of the Oxygen Permeability and Diffusion Coefficient of Hemoglobin in Hemoglobin Solution

The quantity to be directly measured in oxygenation experiments is the ratio of the oxygenation time (t_1) and

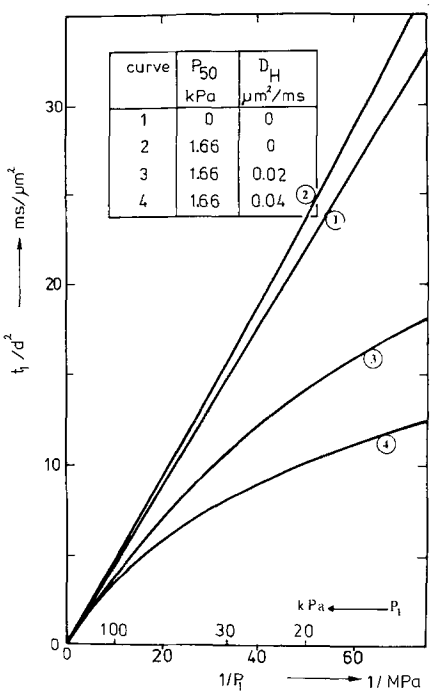

Fig. 6. The normalized oxygenation time (t_1/d^2) as a function of the reciprocal oxygen driving pressure ($1/P_1$) and the influence of both saturation curve and diffusion of oxyhemoglobin on this relationship. $h = 1.24 \cdot 10^{-3}$ mol/([Hb] = 200 g/l), $\alpha = 11.5 \cdot 10^{-9}$ mol·l^{-1}·Pa^{-1}, $D_C = 1.2$ µm²/ms, $P_{50} = 1.66$ kPa. Curve *1*: no influence of saturation curve ($P_{50} = 0$ and $D_H = 0$); *2*: influence of saturation curve and $D_H = 0$; *3*: influence of saturation curve and $D_H = 0.02$ µm²/ms; *4*: as curve *3* but $D_H = 0.04$ µm²/ms

the square of the layer thickness, which is called the normalized oxygenation time:

$$t_1/d^2 = t_1^*/D_C. \tag{15}$$

The dimensionless oxygenation time t_1^* is proportional to H [eq. (14)] which in turn is proportional to $1/P_1$ by definition.

The aim of this study is to estimate values for the diffusion coefficients of oxygen and hemoglobin by fitting the theoretically calculated t_1/d^2 to the measured t_1/d^2 for various values of $1/P_1$. The dependence of the normalized oxygenation time [eqs. (10) and (15)] on $1/P_1$ can be obtained by expressing eq. (14) in absolute quantities for the situation where $S_1 \simeq 1$ and $S_i = 0$:

$$t_1/d^2 = \tfrac{1}{2} f_1\left(P_{50}, \frac{h}{\alpha}, Z\, D_H \frac{1}{P_1}\right) f_2\left(Z\, D_H \frac{1}{P_1}\right) Z \frac{1}{P_1}$$

$$\text{where } Z = \frac{h}{\alpha D_C}. \tag{16}$$

When knowing P_{50} and h/α the parameters Z and D_H can be estimated by the fitting procedure. Accurate knowledge of P_{50} and h/α is not needed since f_1 is only slightly influenced by large variations of parameters. However, for the determination of the diffusion coefficient of oxygen from the estimated value of Z, the values of h and α should be known accurately, whereas for the determination of the oxygen permeability, αD_C, only h should be known well.

The characteristic influences of the saturation curve and the diffusion coefficient of hemoglobin on the relationship between t_1/d^2 and $1/P_1$ are shown in Fig. 6. This figure and eqs. (14) and (16) lead to the following conclusions:

1. If a) there is no influence of the saturation curve on the oxygenation process, b) hemoglobin molecules are immobile, and c) P_1 is varied in a range where S_1 remains close to unity, then the relationship between t_1/d^2 and $1/P_1$ will be linear (curve 1 in Fig. 6).

2. The influence of the saturation curve, while still assuming $D_H = 0$, leads to a concave shape of the t_1/d^2 versus $1/P_1$ curve (curve 2 in Fig. 6).

3. The carrier facilitation as a result of the diffusion of hemoglobin (D_H) leads to a convex shape of the t_1/d^2 versus $1/P_1$ curve (curves 3 and 4 in Fig. 6).

Thus from t_1/d^2 measured as a function of $1/P_1$ both the oxygen permeability and the diffusion coefficient of hemoglobin can be derived. However, some difficulties arise at very low P_1 values, e.g., with P_1 less than five times P_{50}. Figure 1 shows that the linear portion of the plot of $\bar{\Psi}$ against $\sqrt{t^*}$ reaches less far with decreasing P_1 and therefore the determination of t_1/d^2 will be less accurate using the semi-infinite approach. An even more serious reservation against applying low P_1 values is a more marked influence of the saturation curve on the oxygenation process. Referring to Fig. 5, it may be estimated that with Φ_{50} ($\simeq P_{50}/P_1$) below 0.2 the term in eq. (16) for the saturation curve (f_1) varies by only 5%, i.e., the results will not be much affected by changes or inaccuracies in the saturation curve and h/α. With lower values of P_1 (i.e., higher values of Φ_{50}), however, the results will be more influenced by the position of the saturation curve. For these two reasons the use of low values of P_1 (high values of Φ_{50}) should be avoided.

The parameter Z contains the product αD_C being the permeability for oxygen of the hemoglobin solution. Hence, knowing the oxygen binding capcity of the solution the permeability αD_C can be derived. The diffusion coefficient of oxygen D_C can then be calculated knowing the solubility α.

Figure 4 shows that the sensitivity of the detection of hemoglobin-facilitated oxygen transfer (expressed by f_2) depends on the range of D^*. Due to the hyperbolic shape of the plot of f_2 against D^* the value of f_2 will change less with altered D^* in the range of increasing D^* (which is proportional to D_H and $1/P_1$).

Based on this analysis and on published values of D_H a range of P_1 values between 93.1 and 16 kPa (700 and 120 mm Hg), or of $1/P_1$ values between 10.7 and

62.5 MPa^{-1} ($1.4 \cdot 10^{-3}$ and $8.33 \cdot 10^{-3}$ mm Hg^{-1}) seems to be an appropriate compromise.

Evaluation of the "Polygonal Approximation"

When aiming only at an estimate of the values of the physical constants by curve fitting, in general sophisticated theoretical models are not very efficient with respect to computer time. Therefore the polygonal approximation of the saturation curve, as presented by Curl and Schultz (1973) and discussed in more detail by Spaan (1976), has been chosen as a simplified model.

In the polygonal model the saturation curve is approximated by straight line segments. Within these segments $d^2\Psi/d\Phi^2 = 0$ (Appendix eq. A6), and the differential equations describing the semi-infinite layer model of oxygen uptake [eq.(5)] can be solved analytically in terms of error functions.

The results of the polygonal model depend on the choice of the approximation of the saturation curve. Curl and Schultz suggested to quantitatively minimize the area between the saturation curve and the straight line segments. However, this suggestion does not always work well as demonstrated by the straight line approximation (broken line) of curve 2 in Fig. 2 according to Curl and Schultz. The computer solution using this curve 2 yields $t_1^* = 12.7$ ($H = 100$, $D^* = 3$), whereas the straight line approximation yields $t_1^* = 19.8$.

In our situation of relatively low values of Φ_{50}, the polygonal approximation of the dimensionless saturation curve consists of two segments. The first line originates from the point $\Phi = \Psi = 0$ and intercepts the line of final saturation $\Psi = 1$ at the value $\Phi = \Phi_C$. The second line continues to the end point $\Phi = \Psi = 1$. The value of Φ_C (0.2945; see Fig. 2, curve 3) has been chosen such that t_1^* calculated according to the numerical solution of the semi-infinite layer model equals the value obtained from the polygonal approximation using $H = 100$, $D^* = 0.6$ and $\Phi_{50} = 0.1337$. Any change in Φ_{50} was accounted for by a proportional change in Φ_C according to $\Phi_C/\Phi_{50} = 0.2945/0.1337 = 2.203$. This approximate approach holds for the range of Φ_{50}, D^* and H pertaining to our experiments to within 1%.

Contrary to previous approaches where the moving boundary equations were derived using the time and place variables separately (e.g. Danckwerts, 1950; Curl and Schultz, 1973; Crank, 1975), the problem is simplified here by combining the dimensionless variables of place x^* and time t^* into one single variable $\eta = x^*/\sqrt{t^*}$. Due to the early introduction of η the number of physical boundary conditions is restricted since they can only be defined at fixed values of η. Time and place corresponding to fixed values of η are $x^* = 0$, equivalent to $t^* = \infty$, and $t^* = 0$, equivalent to $|x^*| = \infty$, and moreover those interfaces which change position according to $x^*/\sqrt{t^*} = \text{constant}$. The differences in the mathematical treatment of a particular physical problem obviously depend on the specific boundary conditions.

Conclusions

By comparing the semi-infinite and finite model, the oxygenation process can be described by a single number (t_1^* = dimensionless saturation time), which simplifies the presentation of numerical results. Fortunately the influence of the dimensionless saturation curve (Φ_{50}) appears to be minor and, even better, is uniform over a wide range of values of the oxygen concentration ratio and oxygen flux ratio ($25 \leq H \leq 100$, $0.2 \leq D^* \leq 0.8$) in the range covered. Moreover, in case of a rectangular saturation curve ($\Phi_{50} = 0$) the dimensionless oxygenation time appears to be a linear function of H for all values of D^* studied (Fig. 3), where the influence of the oxygen flux ratio (D^*) on the dimensionless oxygenation time at $\Phi_{50} = 0$ ($= t_1^{*,0}$) reflects in the slope of the $t_1^{*,0}$ versus H curves. This parametric analysis thus describes the oxygenation process by three diagrams for its dependence on H, D^* and Φ_{50} respectively (Figs. 3–5). From these relationships the explicit factors of αD_C and D_H may be obtained.

In a companion paper the oxygenation of layers of hemoglobin solutions will be studied experimentally and the determinant factors of this process will be derived.

List of Symbols

C = $C(x, t)$ = oxygen concentration within the hemoglobin layer (mol/l)
C_i = αP_i = initial oxygen concentration (mol/l)
C_1 = αP_1 = final oxygen concentration (mol/l)
d = layer thickness (μm)
D^* = $H\frac{D_H}{D_C}$ = oxygen flux ratio = ratio of carrier-mediated to free oxygen flux at steady state (dimensionless)
D_C = diffusion coefficient of dissolved oxygen (μm^2/ms)
D_H = diffusion coefficient of hemoglobin (μm^2/ms)
f_1 = $t_1^*/t_1^{*,0}$ = factor characterizing the influence of dimensionless saturation curve on dimensionless oxygenation time (dimensionless)
f_2 = nonsteady-state facilitation factor (dimensionless)
F = $\int_0^\eta \Psi(\eta)\, d\eta$
H = $\frac{(S_1 - S_i)\, h}{C_1 - C_i}$ = oxygen concentration ratio = ratio of bound to physically dissolved oxygen after equilibrium (dimensionless)
h = total oxygen binding capacity of the deoxygenated hemoglobin solution (mol/l)
[Hb] = hemoglobin concentration (g/l)

pH = acidity of the solution
P_i = initial oxygen partial pressure (kPa)
P_{CO_2} = partial pressure of carbon dioxide (kPa)
P_{O_2} = partial pressure of oxygen (kPa)
P_1 = final oxygen partial pressure or oxygen driving pressure (kPa)
P_{50} = P_{O_2} where hemoglobin is half saturated with oxygen (kPa)
ΔP = $P_1 - P_i$ = oxygen driving pressure difference across a layer of hemoglobin solution at steady-state oxygen transfer (kPa)
S = $S(x,t)$ = fractional oxygen saturation
S_i = initial fractional oxygen saturation
S_1 = final fractional oxygen saturation
ΔS = $S_1 - S_i$ = fractional oxygen saturation difference across a layer of hemoglobin solution at steady-state oxygen transfer
t = time (s)
t_1 = oxygenation time defined by semi-infinite layer model (s)
t^* = tD_C/d^2 = dimensionless time
t_1^* = dimensionless oxygenation time defined by semi-infinite layer model
$t_1^{*,0}$ = as t_1^* but applying a rectangular saturation curve ($\Phi_{50} = 0$)
t_1/d^2 = normalized oxygenation time independent of layer thickness
x = distance from liquid-gas interface (μm)
x^* = x/d = dimensionless distance from liquid-gas interface
Z = $h/\alpha D_C$ = parameter to be estimated by fitting theory to experimental t_1/d^2 versus $1/P_1$ curve
α = solubility of oxygen in the solution (mol/l/kPa)
η = $\frac{x^*}{\sqrt{t^*}}$ independent dimensionless variable used in the semi-infinite layer model
η_C = value of η where $\Phi = \Phi_C$ and $\Psi = \Psi_C$ in the polygonal approximation
Φ = $\frac{C - C_i}{C_1 - C_i}$ = dimensionless oxygen concentration
Φ_{50} = dimensionless half-saturation oxygen pressure characterizing the position of the dimensionless saturation curve
Φ_C = abscissa value of intercept point of polygonal approximation of the saturation curve
Ψ = $\frac{S - S_i}{S_1 - S_i}$ = dimensionless oxygen saturation
Ψ_∞ = as Ψ but calculated according to the semi-infinite layer model
$\bar{\Psi}$ = space-average dimensionless oxygen saturation of a hemoglobin layer with finite thickness
$\bar{\Psi}_\infty$ = as $\bar{\Psi}$ but calculated according to the semi-infinite layer model

Appendix

The equation holding for the semi-infinite layer model was derived from eq. (1) by the transformation:

$$\eta = \frac{x^*}{\sqrt{t^*}} = \frac{x}{\sqrt{tD_C}} \quad (A1)$$

Because of eq. (A1) one may write:

$$\frac{\partial}{\partial x^*} = \frac{d}{d\eta}\frac{\partial \eta}{\partial x^*} = \frac{1}{\sqrt{t^*}}\frac{d}{d\eta}$$

and

$$\frac{\partial^2}{\partial x^{*2}} = \frac{\partial}{\partial x^*}\left(\frac{1}{\sqrt{t^*}}\frac{d}{d\eta}\right) = \frac{d}{d\eta}\left(\frac{1}{\sqrt{t^*}}\frac{d}{d\eta}\right)\frac{\partial \eta}{\partial x^*} = \frac{1}{t^*}\frac{d^2}{d\eta^2} \quad (A2)$$

and also

$$\frac{\partial}{\partial t^*} = \frac{d}{d\eta}\frac{\partial \eta}{\partial t^*} = -\tfrac{1}{2}\frac{x^*}{\sqrt{t^*}} \cdot \frac{1}{t^*}\frac{d}{d\eta} = -\tfrac{1}{2}\frac{\eta}{t^*}\frac{d}{d\eta} \quad (A3)$$

Substitution of eqs. (A2) and (A3) into eq. (1) yields eq. (5).

In order to use a standard integration procedure eq. (5) was modified by

$$\frac{d\Psi}{d\eta} = \frac{d\Psi}{d\Phi} \cdot \frac{d\Phi}{d\eta} \quad (A4)$$

and

$$\frac{d^2\Psi}{d\eta^2} = \frac{d\Psi}{d\Phi}\frac{d^2\Phi}{d\eta^2} + \frac{d^2\Psi}{d\Phi^2}\left(\frac{d\Phi}{d\eta}\right)^2 \quad (A5)$$

into

$$\frac{d^2\Phi}{d\eta^2} = \frac{-1}{\left(1 + D^*\frac{d\Psi}{d\Phi}\right)}\frac{d\Phi}{d\eta}\left[\tfrac{1}{2}\eta\left(1 + H\frac{d\Psi}{d\Phi}\right) + D^*\frac{d^2\Psi}{d\Phi^2}\frac{d\Phi}{d\eta}\right] \quad (A6)$$

For the calculation of t_1^* the integral $\int_0^\infty \Psi\, d\eta$ is needed. This integral has been solved as follows. First F is defined as:

$$F \equiv \int_0^\eta \Psi(\eta)\, d\eta \quad (A7)$$

Twofold derivation of (A7) leads to:

$$\frac{dF}{d\eta} = \Psi(\eta) \quad (A8)$$

$$\frac{d^2F}{d\eta^2} = \frac{d\Psi}{d\eta} = \frac{d\Psi}{d\Phi}\frac{d\Phi}{d\eta}. \quad (A9)$$

Eqs. (A6) and (A9) form a set of two differential equations which have been solved simultaneously by a fourth-order Runge-Kutta integration procedure (Library program of the Computing Centre of the Eindhoven University of Technology) resulting in Φ and F as a function of η where $1/F^2 = t_1^*$ for $\eta \to \infty$.

The integration procedure requires two different boundary conditions per differential equation at $\eta = 0$,

i.e. Φ $(\eta = 0)$, $\Psi(\eta = 0)$, $(d\Phi/d\eta)_{\eta=0}$, and $(d\Psi/d\eta)_{\eta=0}$. The latter two replace the physical boundary conditions $\Phi \to 0$ and $\Psi \to 0$ when $\eta \to \infty$.

The boundary conditions for Ψ are determined by the boundary conditions for Φ by the saturation curve. A parameter estimation program has been developed in order to determine the particular value of $(d\Phi/d\eta)_{\eta=0}$ satisfying the boundary condition $\Psi \to 0$ when $\eta \to \infty$.

All errors involved, including the truncation error by stopping the integration at a finite value of η, add up but remain within $\pm$ 0.2 % of the calculated value of t_1^*. For a discussion of this point see Spaan (1976).

The authors greatly appreciate the generous cooperation and stimulation by Prof. Dr. P. C. Veenstra in this work.

References

Crank, J.: The mathematics of diffusion. Second Edition. Oxford: Clarendon Press 1975

Curl, R. L., Schultz, J. S.: A polygonal approximation for unsteady state diffusion of oxygen into hemoglobin solutions. In: Oxygen transport to tissue. Pharmacology, mathematical studies, and neonatology. (D. F. Bruley, H. I. Bicher, eds.), pp. 929–935. Adv. Exper. Med. Biol. Vol. 37B. New York-London: Plenum Press 1973

Danckwerts, P. V.: Unsteady-state diffusion or heat conduction with moving boundary. Trans. Faraday Soc. **46**, 701–712 (1950)

Dindorf, J. A., Lightfoot, E. N., Solen, K. A.: Prediction of blood oxygenation rates. Chem. Eng. Symp. Ser. **67**, 75–87 (1971)

Hill, A. V.: The diffusion of oxygen and lactic acid through tissues. Proc. Roy. Soc. B **104**, 39–96 (1928/29)

Klug, A., Kreuzer, F., Roughton, F. J. W.: The diffusion of oxygen in concentrated haemoglobin solutions. Helv. Physiol. Pharm. Acta **14**, 121–128 (1956)

Kreuzer, F.: Über die Gültigkeit des Fickschen Gesetzes bei der Diffusion des Sauerstoffs in dünnen Schichten hochkonzentrierter Hämoglobinlösungen. Thesis, Fribourg-Zürich 1950

Kreuzer, F.: Modellversuche zum Problem der Sauerstoffdiffusion in den Lungen. Helv. Physiol. Pharm. Acta **11**, Suppl. 9 (1953)

Kreuzer, F., Hoofd, L. J. C.: Facilitated diffusion of oxygen in the presence of hemoglobin. Respir. Physiol. **8**, 280–302 (1970)

Kreuzer, F., Hoofd, L. J. C.: Factors influencing facilitated diffusion of oxygen in the presence of hemoglobin and myoglobin. Respir. Physiol. **15**, 104–124 (1972)

Kutchai, H.: O_2 uptake by 100 μ layers of hemoglobin solution. Theory vs experiment. Respir. Physiol. **11**, 378–383 (1971a)

Kutchai, H.: Wider applicability for Hill's advancing front theory of oxygen uptake. J. Appl. Physiol. **31**, 302–304 (1971b)

Marx, T. I., Snyder, W. E., St. John, A. D., Moeller, C. E.: Diffusion of oxygen into a film of whole blood. J. Appl. Physiol. **15**, 1123–1129 (1960)

Mikic, B. B., Benn, J. A., Drinker, P. A.: Upper and lower bounds on oxygen transfer rates: a theoretical consideration. Ann. Biomed. Eng. **1**, 212–220 (1972)

Moll, W.: The influence of hemoglobin diffusion on oxygen uptake and release by red cells. Respir. Physiol. **6**, 1–15 (1968/69)

Spaan, J. A. E.: Transfer of oxygen into haemoglobin solution. Pflügers Arch. **342**, 289–306 (1973)

Spaan, J. A. E.: Oxygen transfer in layers of hemoglobin solution. Ph. D. Thesis, Eindhoven University of Technology, The Netherlands, 1976

Thews, G.: Ein Verfahren zur Berechnung des O_2-Diffusionskoeffizienten aus Messungen der Sauerstoffdiffusion in Hämoglobin- und Myoglobin-Lösungen. Pflügers Arch. **265**, 138–153 (1957)

Weissman, M. H., Mockros, L. F.: Oxygen and carbon dioxide transfer in membrane oxygenators. Med. Biol. Eng. **7**, 169–184 (1969)

Received November 6, 1978/Accepted November 22, 1979